

Next-Generation MPPT Algorithms for Integrated Wind and Photovoltaic Power Systems

S. Anibabu¹, Mr.P. Mahesh², Dr.R.S.R. Krishnam Naidu³

¹*M.Tech Student, Department of EEE, Nadimpalli Satyanarayana Raju Institute of Technology, Sontyam, Visakhapatnam, India*

²*Assistant Professor, Department of EEE, Nadimpalli Satyanarayana Raju Institute of Technology, Sontyam, Visakhapatnam, India*

³*Professor & HOD, Department of EEE, Nadimpalli Satyanarayana Raju Institute of Technology, Sontyam, Visakhapatnam, India*

Abstract—Conventional maximum power point tracking (MPPT) techniques in wind energy conversion systems (WECS), such as the perturb and observe (P&O) algorithm, often struggle with dynamic response and steady-state oscillations due to fixed step size limitations. This paper presents an enhanced MPPT approach that combines fuzzy logic control with the trapezoidal rule to improve tracking performance. The proposed method is benchmarked against the conventional P&O and trapezoidal rule-based P&O (TRPO) algorithms using MATLAB/Simulink under stochastic wind profiles. Simulation results reveal that the hybrid fuzzy–trapezoidal method effectively reduces power oscillations and enhances the stability and efficiency of power output. Additionally, the methodology is extended to a wind–solar hybrid energy system by integrating an artificial neural network (ANN)-based controller. This hybrid system demonstrates improved performance in terms of maximum power extraction, stability, and adaptability to fluctuating environmental conditions

I. OVERVIEW

The global demand for energy has escalated significantly due to rapid industrialization, rising living standards, and population growth. This surge in consumption has accelerated the depletion of conventional fossil fuel resources such as coal, gas, and oil. In response, the transition toward renewable energy sources has become imperative for ensuring long-term sustainability. Among the available options, wind energy has emerged as a promising and environmentally friendly solution. Wind Energy Conversion Systems (WECS) are designed to harness

kinetic wind energy and convert it into electrical power using wind turbines (WT) and associated power electronics. However, the inherently variable nature of wind poses a critical challenge: efficiently capturing and converting fluctuating wind energy into stable electrical output. The primary function of a wind turbine is to extract kinetic energy from the wind and convert it into mechanical energy through rotor blades, which is subsequently transformed into electrical energy via a generator. Several generator types are employed in WECS, each with its own benefits and drawbacks. The Squirrel Cage Induction Generator (SCIG) is known for its simplicity, cost-effectiveness, and high reliability, but it requires external excitation and offers relatively low efficiency. The Doubly Fed Induction Generator (DFIG), on the other hand, operates efficiently with partial-scale converters and is considered a cost-effective solution compared to SCIG. However, its reliance on a multi-stage gearbox and excitation system increases system complexity. Permanent Magnet Synchronous Generators (PMSG) are gaining popularity due to their self-exciting nature, high reliability, and compact design, making them suitable for modern wind energy systems. A major factor affecting WECS performance is the variability of wind speed, which leads to fluctuations in power output. To optimize power generation under these dynamic conditions, Maximum Power Point Tracking (MPPT) techniques are essential. MPPT algorithms continuously adjust system parameters to ensure operation at the optimal power point. These techniques are broadly categorized into three types.

WT parameter-based methods, such as Tip Speed Ratio (TSR) and Optimal Torque Control (OTC), require detailed knowledge of turbine characteristics. Sensor less methods, such as the widely adopted Perturb and Observe (P&O) algorithm, eliminate the need for wind speed sensors but may suffer from lower tracking efficiency. Hybrid methods aim to combine the strengths of both approaches to enhance overall performance. The P&O algorithm remains popular due to its simplicity and minimal sensor requirements. However, it faces a major drawback: selecting the appropriate step size. A large step size enables faster convergence to the Maximum Power Point (MPP) but induces significant power oscillations, while a small step size improves stability but slows convergence, potentially leading to suboptimal energy capture. To address these limitations, researchers have proposed several enhanced MPPT strategies. Modified P&O (MPO) techniques incorporate adaptive features, such as Power Signal Feedback (PSF), Optimal Relation-Based (ORB) methods, and adaptive step-size algorithms, to improve convergence speed and accuracy. Fuzzy Logic Control (FLC) introduces intelligent, rule-based decision-making that dynamically adjusts system parameters in response to input changes, offering superior adaptability in uncertain environments. Additionally, Artificial Neural Networks (ANN) and metaheuristic optimization algorithms have been applied to MPPT, showing potential for high accuracy and learning capabilities. However, these methods often involve increased computational requirements and complexity, posing challenges for real-time implementation in embedded systems.

D. Proposed Hybrid MPPT Approach

To overcome the inherent limitations of conventional, Perturb and Observe (P&O) methods—particularly in terms of step size sensitivity and tracking accuracy—this study introduces a hybrid MPPT strategy that combines Fuzzy Logic Control (FLC) with the Trapezoidal Rule. In the proposed method, the trapezoidal rule is utilized to accurately extract real-time maximum power and voltage values from the rectified current and voltage signals. These values provide a reliable reference for the fuzzy logic controller, which dynamically determines the appropriate duty cycle required for efficient

Maximum Power Point (MPP) tracking. Unlike the fixed-step P&O algorithm, the fuzzy logic component adapts to system variations, enabling more precise and stable tracking of the MPP under fluctuating wind conditions.

II. CONNECTED IDEAS

Figure 1 presents the block diagram of a typical wind energy conversion system. Based on the Betz limit, a wind turbine can theoretically extract no more than 59% of the kinetic energy available in the wind. The wind turbine (WT) captures this energy by converting the kinetic motion of air into mechanical power. The mechanical power output (P_m) from the turbine is determined using Equation (1), which depends on the characteristics of the wind and the turbine design. The power available in the wind, often referred to as P_w , is described in Equation (2). It is a function of air density (ρ), wind speed (V) in meters per second, and the swept area (A) covered by the turbine blades, expressed in square meters (m^2). The swept area itself is calculated based on the blade radius (R), as shown in Equation (3). Additional parameters critical to wind energy conversion include the power coefficient (C_p), which reflects the efficiency of power extraction; the angular velocity (ω) of the rotor, measured in radians per second; and the tip speed ratio (λ), which represents the ratio of blade tip speed to the wind speed. Together, these parameters govern the aerodynamic and mechanical performance of the wind turbine system.

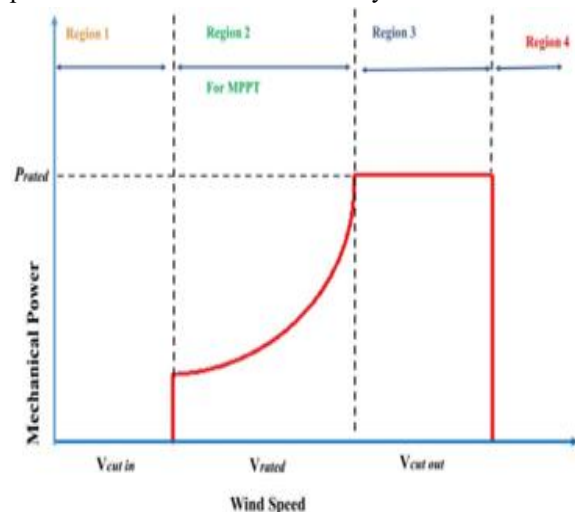
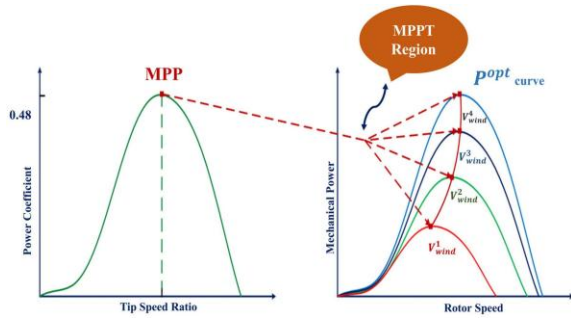
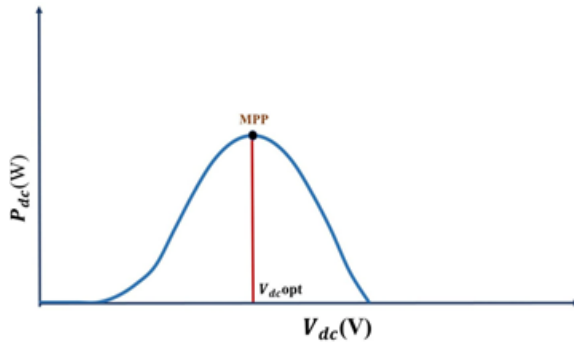


Figure 1. WECS operating regions

Figure 2. WT characteristics for λ_{opt} and $C_{p_{opt}}$.Figure 3. Relation between V_{dc} and P_{dc} .

The power available in the wind, often referred to as P_{air} , represents the total energy contained in the wind as well as the portion absorbed by the wind turbine. According to the Betz limit, the maximum power that can be captured by a wind turbine is restricted to 59% of this available power, as indicated in Equation (4). Equations (1) through (4), which define the relationships between wind speed, power, and turbine efficiency, are referenced from [26]. In a typical Wind Energy Conversion System (WECS), the wind turbine first converts the kinetic energy of the wind into mechanical energy, which is then delivered to the generator stage. This generator converts mechanical energy into electrical energy, producing a three-phase AC output. This output is subsequently fed into a three-phase rectifier, which transforms the AC into DC voltage. To optimize the energy output, the system employs a Maximum Power Point Tracking (MPPT) algorithm that controls a DC-DC boost converter. The algorithm calculates the optimal duty cycle, which is sent to a Pulse Width Modulation (PWM) generator. The PWM signal regulates the switching element of the boost converter, adjusting the voltage level and thereby maximizing the power output. The various operating regions of WECS output power are illustrated in

Figure 2. The first region represents conditions where the wind speed is too low for the turbine to generate electricity. The second region, lying between the cut-in wind speed and the rated wind speed, is critical for control strategies aimed at extracting maximum power. The third region, which spans from the rated wind speed to the cut-out wind speed, focuses on protecting the system from overloading while maintaining stable output. Finally, the fourth region includes wind speeds above the cut-out threshold, during which the system is typically shut down to prevent mechanical damage and ensure safety.

$$P_m = \frac{1}{2} \rho A V^3 C_p(\lambda, \beta) \quad (1)$$

$$P_{air} = \frac{1}{2} \rho A V^3 \quad (2)$$

$$\lambda = \frac{R \omega}{V} \quad (3)$$

$$C_p = \frac{P_{windturbine}}{P_{air}} \quad (4)$$

The second operating region—between the cut-in and rated wind speeds—is the primary focus of this study, as it is within this range that the Maximum Power Point Tracking (MPPT) technique is most effective for optimizing the power output of the Wind Energy Conversion System (WECS). This region allows the system to operate below its rated capacity, enabling real-time adjustments for maximum energy extraction. As illustrated in Figure 3, the MPPT control strategy is designed to ensure that the WECS operates along its optimal power curve, where the power output is maximized for a given wind speed. By continuously adjusting the system parameters, the MPPT algorithm enables the WECS to track and maintain operation at the Maximum Power Point (MPP). Consequently, this approach not only enhances overall system efficiency but also ensures the reliable and consistent capture of wind energy under varying environmental conditions. The effectiveness of the Conventional Perturb and Observe (CPO) method in tracking the Maximum Power Point (MPP) largely depends on the selection of the appropriate step size. A small step size ensures accuracy but slows down convergence, whereas a large step size speeds up tracking but introduces oscillations around the MPP—creating a clear trade-off. The proposed method addresses this limitation by integrating the trapezoidal rule with fuzzy logic control (FLC), offering a more adaptive and accurate approach. As illustrated in Figure 4, the relationship between DC voltage (V_{dc}) and DC power (P_{dc})

highlights that an optimal value of V_{dc} corresponds to the maximum P_{dc} (i.e., the MPP). This relationship serves as the foundation for the proposed technique. The method is carried out in three stages, as outlined in Figure 5.

In the first stage, the V_{dc} – P_{dc} curve is divided into equal-width segments using the trapezoidal rule, effectively breaking the curve into trapezoids. During the second stage, the areas of current and previous trapezoids are compared to identify the segment that yields maximum power output, as shown in Figure 7. The third stage uses this information to implement the Fuzzy Logic Controller (FLC) to track the MPP. The FLC structure, depicted in Figure 8, takes as inputs the output power (P_{out}) and voltage (V_{out}) resulting from the trapezoidal rule application. The controller computes two parameters: the error (e) and the change in error (ec), derived from the ratios of δP and δV , as defined in Equations (5) and (6). The FLC inputs " e " and " ec " are further specified in Equations (7), (8), and (9). The system uses Mamdani-type fuzzy inference system (FIS), with minimum (min) and maximum (max) operations for implication and aggregation, respectively. Defuzzification is performed using the centroid method, ensuring smooth and accurate control signal generation

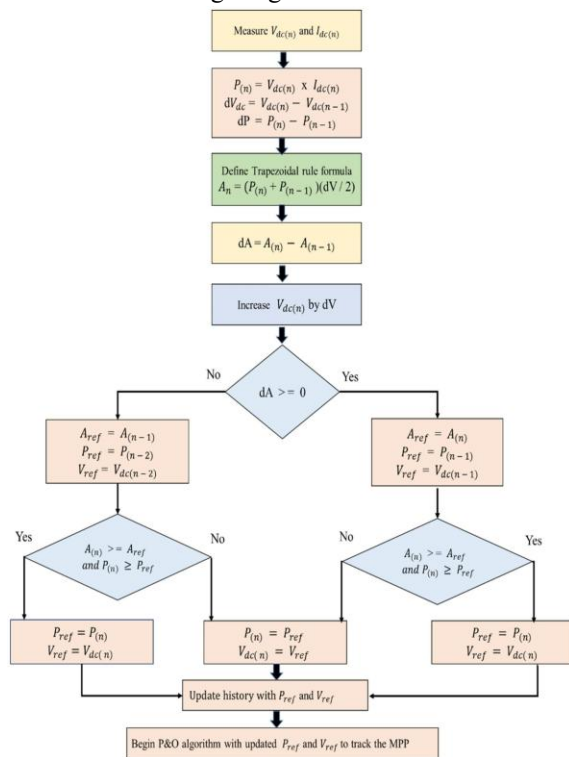


Figure 4. Procedure of the proposed MPPT method.

FLC has the ability to properly track variations in wind speed. The inputs " e " and " ec ," which are sent to the controller, are fuzzed to create the fuzzy set. In order to provide the proper fuzzy output, the inference system uses the fuzzy rules to process the fuzzy set. Following defuzzification, the fuzzy output is ultimately transformed to the duty cycle, which is then utilized to further regulate the boost converter's switching element and enable MPP tracking.

$$\delta P = P_{(n)} - P_{(n-1)} \quad (5)$$

$$\delta V = V_{(n)} - V_{(n-1)} \quad (6)$$

$$e_{(n)} = \delta P / \delta V \quad (7)$$

$$ec = e_{(n)} - e_{(n-1)} \quad (8)$$

The membership function for the inputs " e ," " ec ," and " D " is displayed in Figures 9, 10, and 11. These membership functions have seven variables defined: Nbig, Nmed, Nsmall, Zero, Psmall, Pmed, and Pbig. The fuzzy rules' intricate reasoning is as follows:

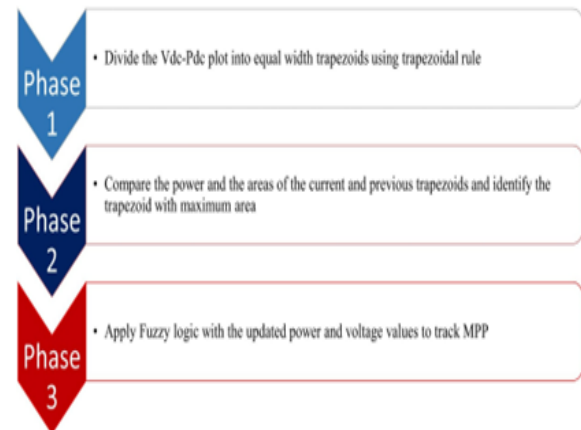


Figure 5. Phases of the proposed technique.

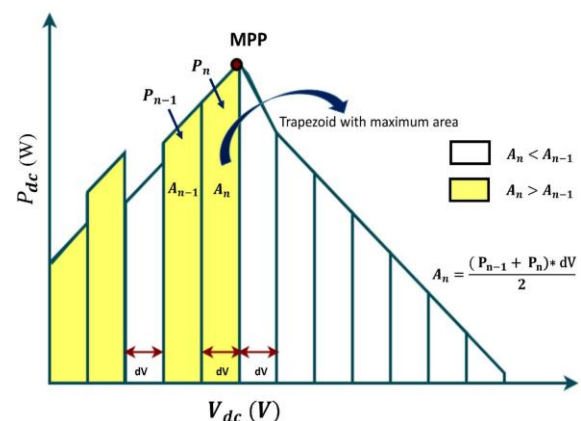


Figure 6. Theme of the proposed technique

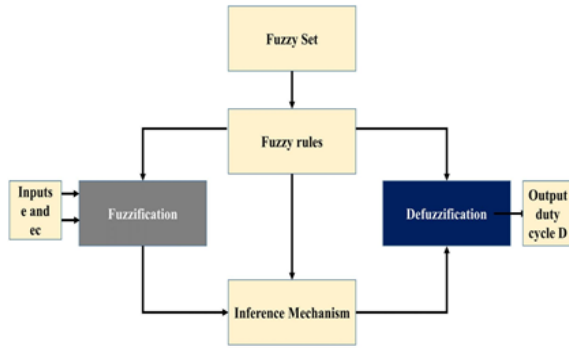


Figure 7. Basic frame work of FLC.
Membership function Plot

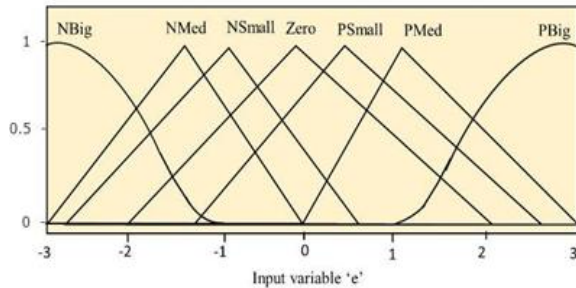


Figure 8. FLC input e membership function

$D = \text{Zero}$ if $e = \text{NBbig}$ and $ec = \text{NBbig}$.

$D = \text{Zero}$ if $e = \text{NBbig}$ and $ec = \text{NMed}$; $D = 0$ if $e = \text{NBbig}$ and $ec = \text{NSmall}$.

Membership function Plot

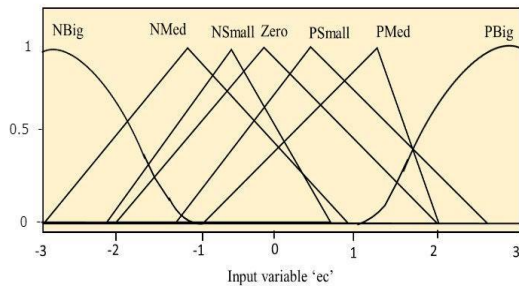


Figure 9. FLC input ec membership function.
Membership function Plot

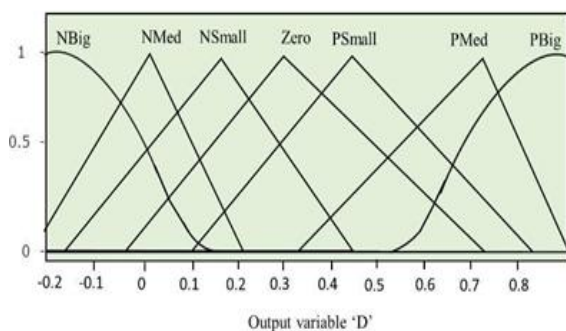


Figure 10. FLC output D membership function.

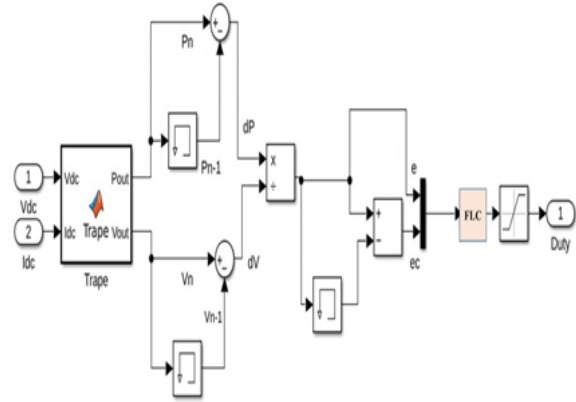


Figure 11. Fuzzy logic applied after trapezoidal rule in the proposed algorithm.

Table 2 displays the 49 rules that are framed for FLC. Figure 12 displays the FLC block diagram that was used during simulation. Figure 5 shows the comprehensive process.

III. CPO SIMULATION AND THE SUGGESTED METHODS

The WECS model with the TRPO, CPO, and suggested trapezoidal rule-based FLC MPPT methods blocks is displayed in Figure 13 and is simulated using MATLAB/Simulink.

The WECS simulates one technique at a time using a manual switch. The simulated system's parameters are shown in Table 3. The Simulink CPO block is displayed in Figure 14. The TRPO method's Simulink model is displayed in Figure 14, and the technique's blocks are shown in Figure 15.

TABLE 2. Rules for FLC.

Output D	Input 'e'							
Input 'ec'		NBig	NMed	NSmall	Zero	PSmall	PMed	PBig
	NBig	Zero	Zero	NSmall	NMed	PSmall	PMed	PBig
	NMed	Zero	Zero	Zero	NSmall	PMed	PMed	PBig
	NSmall	Zero	Zero	Zero	Zero	PMed	PMed	PBig
	Zero	NBig	NSmall	Zero	Zero	PSmall	Zero	Zero
	PSmall	NBig	NMed	NSmall	Zero	Zero	Zero	Zero
	NMed	NBig	NMed	NSmall	PSmall	Zero	Zero	Zero
	PBig	NMed	NMed	NSmall	PMed	Zero	Zero	Zero

TABLE 3. Simulation system parameters.

WT Parameters	Value and Unit
Radius	3.01m
Air density	1.22kg/m ³
Rated Power	1 Kilo Watt
β	0
PMSG Parameters	Value and Unit
Rated Power	1 Kilo Watt
Pole pairs	2
R_s	1.6 Ω
$L_d=L_q$	6.3 milliHenry
J	8.54 kgm ²
Boost Converter Parameters	Value and Unit
L	75 milliHenry
C	0.468 μ Farads
Switching Frequency	5KHz
R_L	54 Ω

The power coefficient for each of the three methods is shown in Figure 17. The random fluctuation in wind speed utilized to simulate all three methods is shown in Figure 18. The suggested technique's curve is shown in red, TRPO's in light blue, and the CPO methods in navy blue. The relative voltage, current, and DC output power attained with each of the three methods are displayed in Figures 19, 20, and 21 correspondingly. These Figures A, B, C, D, and E markings show the improved output power, voltage, and current as well as the decrease in oscillations. These Figures make it clear that the suggested method helps to lessen oscillations and increase the power produced at the output.

IV. OUTCOMES

The TRPO, CPO, and the suggested MATLAB/Simulink approach are all simulated in the preceding section. The power coefficient for each of the three methods is shown in Figure 17. Table 3 provides specifics about the simulated system's specs. Figure 18 illustrates the differences in wind speed. Higher produced voltage, current, and power are shown by the graphs presented in Figures 19, 20, and 21, respectively. The contrast between the TABLE 4. Comparison of the rise time. Response time and the transient time of all the three simulated techniques.

Name of the MPPT algorithm	Rise time (m sec)	Transient time(m sec)	Response time(m sec)
Trapezoidal rule based Fuzzy logic	0.1231	6.9450	0.035
Trapezoidal rule based PO	0.2133	6.9450	0.040
Conventional P & O	0.3200	6.9700	0.060

TABLE 5. Comparison of the tracking efficiency for

all the three techniques at the rated wind speed of 5 m/s.

Name of the MPPT algorithm	MPPT Tracking efficiency
Trapezoidal rule based Fuzzy logic	99.1%
Trapezoidal rule based P & O	92.7%
Conventional P & O	87%

The superiority of the proposed MPPT algorithm is validated by comparative analysis with the Conventional Perturb and Observe (CPO) and Trapezoidal Rule-based Perturb and Observe (TRPO) methods. As illustrated in Figures A, B, C, and D, the proposed approach consistently yields higher output power with reduced oscillations. In the simulation, the wind speed was randomly varied across values of 4, 5, 4, 3, and 5 m/s, where 5 m/s represents the rated wind speed and corresponds to the maximum power output for all methods. The maximum duty cycle observed for the proposed, TRPO, and CPO techniques were 0.37, 0.302, and 0.29, respectively, indicating stronger control and better tracking in the proposed method. As detailed in Table 4, the proposed approach exhibits faster rise time, improved response time, and reduced transient duration when compared with the other two algorithms. The TRPO method, in comparison to CPO, achieves output improvements of 0.6% in voltage, 6.8% in current, and 1.06% in power, further emphasizing the advantage of enhanced tracking mechanisms. Moreover, Table 5 presents the tracking efficiency of each technique, confirming that the proposed method maintains the highest MPP tracking accuracy among all three. Table 6 provides additional performance metrics, reinforcing the overall superiority and robustness of the proposed hybrid MPPT algorithm under wind Conditions

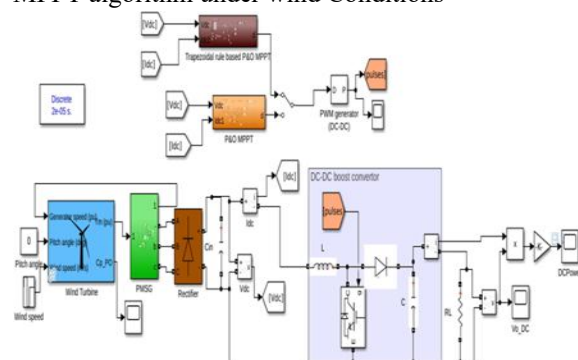


Figure 12. Simulation Model in MATLAB/Simulink for the TRPO, CPO and the proposed algorithm.

TABLE 6. Comparison of the MPPT techniques.

Parameters of the MPPT technique	TSR [15], [45]–[48]	PSF [15], [45], [46]	OT [15], [45]–[48]	CPO [15], [45]–[48]	INC [15], [45]–[48]	ORB [15], [45]–[48]	NN [45], [47]	TRPO [43]	Proposed Technique
Efficiency of Tracking MPP	High	Moderate	Moderate	Low	Low	Moderate	High	High	High
Convergence speed	High	High	High	Low	Low	Medium	High	High	High
Oscillations near the MPP	No	No	No	Yes	Yes	No	No	No	No
Training data requirement	No	Yes	Yes	No	No	No	Yes	No	No
Wind speed estimation sensor requirement	Yes	Yes	No	No	No	No	Depends	No	No
Performance under changing wind speed	High	Moderate	High	Moderate	Moderate	Moderate	High	High	Excellent

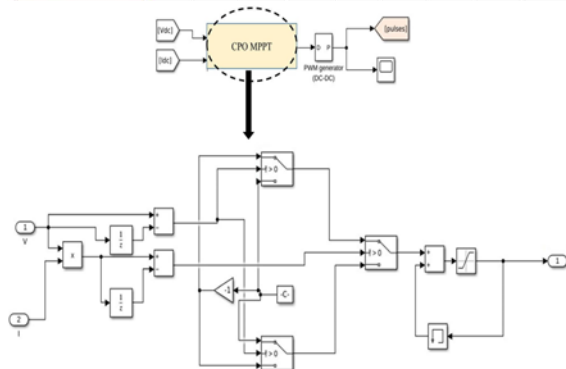


Figure 13. CPO technique SIMULINK block.

improved using the suggested FLC technique based on the Trapezoidal rule, which shows an increase of 8.02% in DC output power, 6.14% in DC output voltage, and 6.14% in DC output current over CPO. The Trapezoidal based FLC methodology, which is the suggested method, produces 5.4%, 5.4%, and 7.36% more

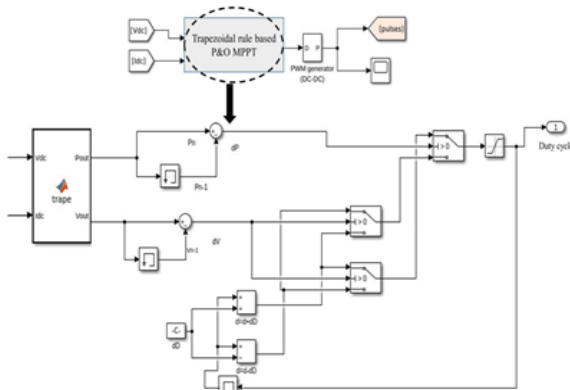


Figure 14. SIMULINK block for TRPO algorithm.

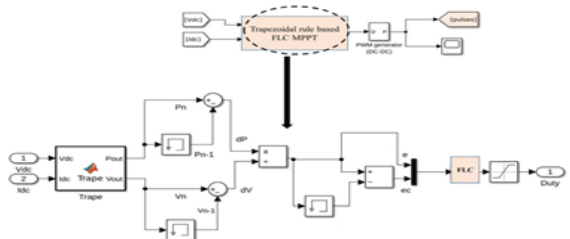


Figure 15. Simulation block for the presented

technique in MATLAB/Simulink.

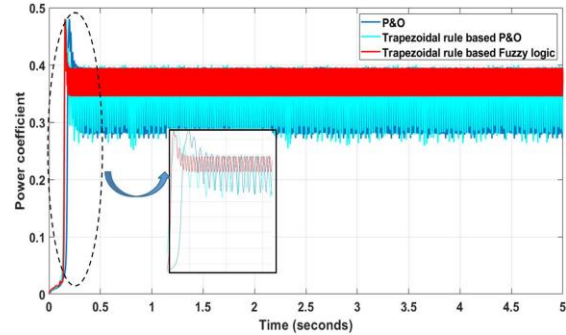


Figure 16. Plot of the Power coefficient

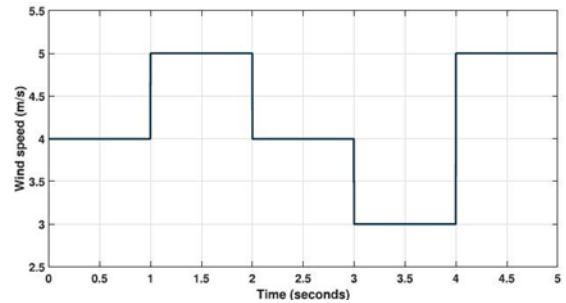


Figure 17. Profile of variation in the wind speed.

V. DISCUSSION

Numerous Maximum Power Point Tracking (MPPT) techniques have been proposed for Wind Energy Conversion Systems (WECS), each offering distinct advantages. However, these methods often involve trade-offs—enhancing one performance metric may compromise another. A key challenge lies in designing an MPPT strategy capable of consistently extracting maximum power under highly variable wind conditions while minimizing oscillations around the Maximum Power Point (MPP) and maintaining low computational complexity. Although optimization-based MPPT methods demonstrate strong tracking performance, they are frequently hindered by significant computational demands, making them less suitable for real-time applications. Hybrid MPPT approaches have emerged as promising alternatives, addressing many of the shortcomings of traditional techniques. Nevertheless, their implementation is often complex and resource intensive. Consequently, there is a clear need for MPPT techniques that are not only effective and accurate but also simple, computationally efficient, and practical for real-time deployment.

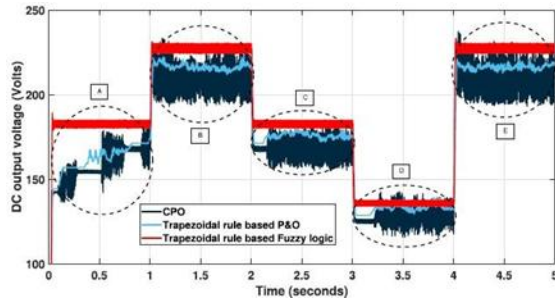


Figure 18. Plot of Time and output Voltage.

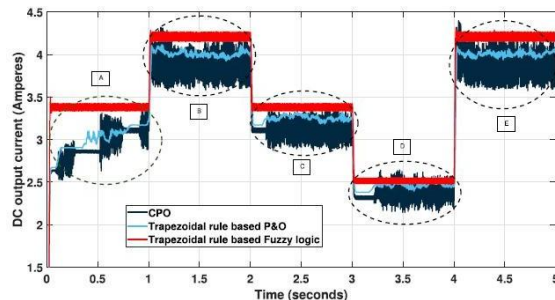


Figure 19. Plot of Time and output Current.

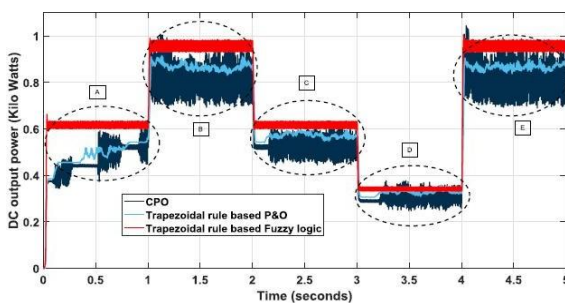


Figure 20. Plot of Time and output Power.

In the proposed hybrid system, a Feedforward Neural Network (FFNN) is employed for Maximum Power Point Tracking (MPPT), effectively addressing the non-linear characteristics of both wind and solar energy sources. The architecture of the FFNN comprises an input layer that receives four key parameters—wind speed (V_w in m/s), solar irradiance (G in W/m^2), photovoltaic (PV) voltage (V_{pv} in V), and PV current (I_{pv} in A). It includes two hidden layers, each consisting of 10 neurons with Rectified Linear Unit (ReLU) activation functions, chosen for their efficiency and ability to prevent vanishing gradient problems. The output layer generates two normalized duty cycles, d_{wind} and d_{solar} (ranging between 0 and 1), which are used to control the wind and solar DC-DC converters, respectively, for optimal power extraction. The

network was trained using 10,000 data samples generated via MATLAB/Simulink simulations, with wind speed ranging from 0 to 25 m/s (in 0.1 m/s steps) and irradiance from 0 to 1000 W/m^2 (in 10 W/m^2 steps). The Adam optimizer was employed for training, configured with a learning rate of 0.001 and standard β_1 , β_2 , and ϵ values. A mini-batch size of 32 was used, and training performance was evaluated using the Mean Squared Error (MSE) loss function, along with 10-fold cross-validation to minimize the risk of overfitting. To improve training efficiency, all input features were normalized to a 0–1 range using min-max scaling.

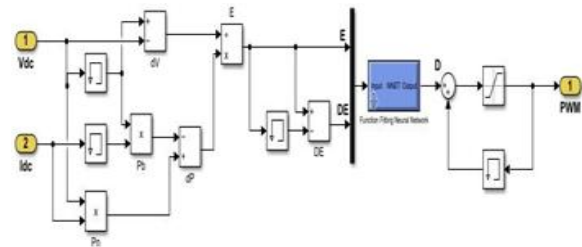


Figure 22: Simulation block for the ANN MPPT

Artificial Neural Networks (ANNs) are particularly effective for Maximum Power Point Tracking (MPPT) in hybrid wind-solar systems due to their ability to model and manage the inherent nonlinearities of such renewable energy sources. Unlike conventional methods, ANNs can adapt to dynamic environmental conditions, such as fluctuating wind speeds and varying solar irradiance, ensuring improved power capture. Compared to Fuzzy Logic Controllers, ANNs offer a data-driven approach that enables them to learn and model complex system behaviors more accurately. Moreover, they provide a balanced trade-off between computational accuracy and real-time performance, unlike metaheuristic algorithms which, though precise, often suffer from high computational demands. In the presented system, MPPT is implemented through a hybrid approach combining the trapezoidal rule with Fuzzy Logic Control (FLC), eliminating the need for wind speed sensors while effectively reducing power oscillations. This integration enhances both tracking speed and power extraction. Figure 21 illustrates a block diagram of the wind energy system based on the Betz limit, which states that no more than 59% of the wind's kinetic energy can be converted into mechanical energy by a wind turbine (WT), as some energy must

remain to allow airflow past the blades. The mechanical power P_m extracted by the turbine is calculated using the equation:

$$P_m = 0.5 \cdot C_p \cdot \rho \cdot A \cdot V^3$$

Where C_p is the power coefficient, ρ is the air density, A is the swept area of the turbine blades, and V is the wind velocity. This foundational principle supports the system's architecture and serves as a baseline for optimizing energy conversion through intelligent MPPT strategies. Future work could explore integrating ANN-based approaches with other numerical and hybrid methods to further enhance efficiency and tracking performance in Wind Energy Conversion Systems (WECS).

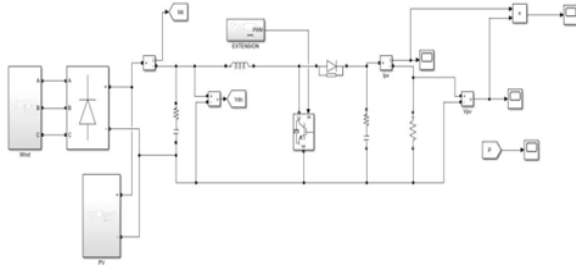


Figure 21: Block diagram of solar and wind with ANN

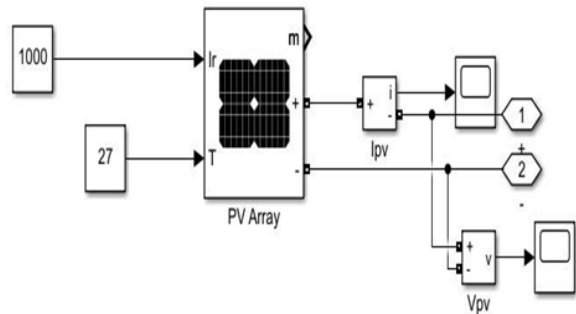


Figure 23: Simulation block for the PV in MATLAB/Simulink.

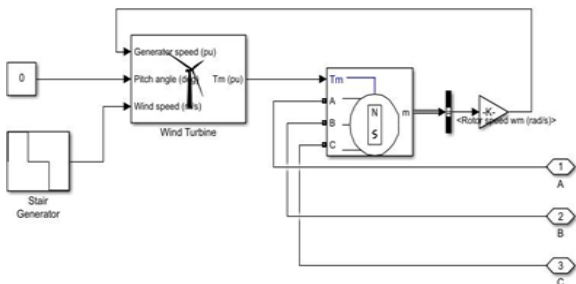


Figure 24: Simulation block for the Wind in MATLAB/Simulink.

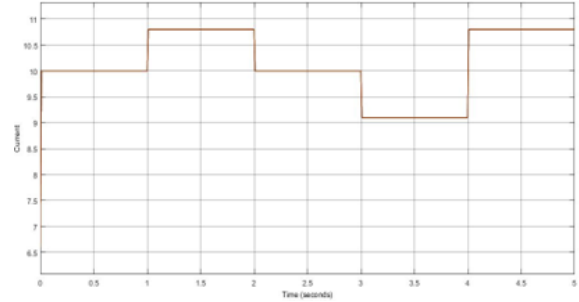


Fig22: Time Vs O/P Current

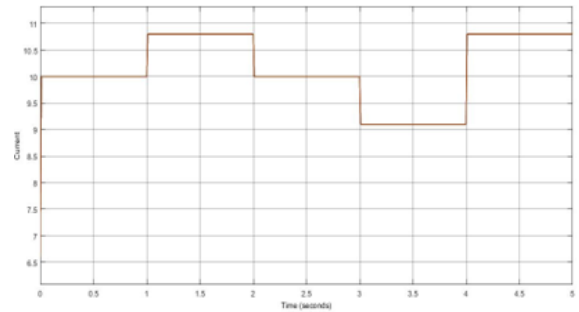


Figure 24: Time Vs Output Voltage

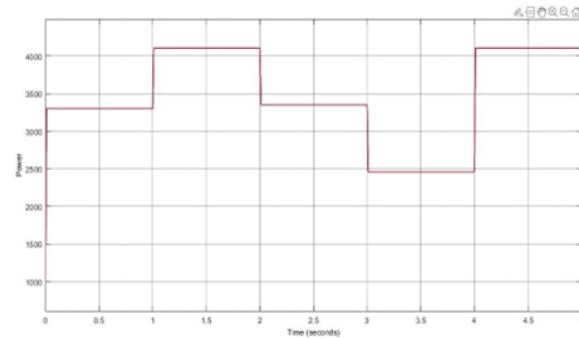


Fig25: Time Vs o/p Power

To improve power generation efficiency, a hybrid wind- solar energy system is employed, combining the outputs of both renewable sources. The integration of an Artificial Neural Network (ANN) enhances the system's performance by enabling adaptive Maximum Power Point Tracking (MPPT). ANN intelligently responds to fluctuating environmental conditions, thereby optimizing energy extraction in real time. The proposed approach utilizes numerical techniques and intelligent control algorithms to maximize power efficiency. In wind energy conversion, the power available in the wind (Pair) and the mechanical power captured by the wind turbine are constrained by the Betz limit, which states that no more than 59% of the wind's kinetic

energy can be converted into usable mechanical power.

Equations related to wind power, turbine swept area, and mechanical conversion are referenced in [26]. The mechanical energy generated by the turbine is converted into electrical energy by a generator. This three-phase output is rectified into direct current (DC) using a three-phase rectifier. An MPPT-controlled DC-DC boost converter, driven by a Pulse Width Modulation (PWM) generator, adjusts the duty cycle to regulate the converter's switching. This increases the DC voltage output, thereby improving the overall energy yield of the system. The wind turbine operates within distinct output power zones, each characterized by varying wind speeds. In Zone 1, wind speeds are too low to generate power. Zone 2 lies between the cut-in and rated wind speeds, where the turbine begins producing power and MPPT plays a critical role in maximizing efficiency. Zone 3 occurs when wind speeds exceed the rated level, causing the turbine's output power to plateau. To further enhance energy generation, a hybrid wind-solar system is adopted, leveraging the complementary nature of both renewable sources. This system incorporates an Artificial Neural Network (ANN) to improve the MPPT process, enabling dynamic adaptation to environmental fluctuations. The wind energy conversion system (WECS) captures kinetic energy using a turbine and generator, while the photovoltaic (PV) system harnesses solar energy through PV panels. The ANN optimizes MPPT for both sources, adjusting the duty cycle in real-time to reduce energy losses and improve tracking accuracy. Selecting an appropriate step size is crucial in MPPT to prevent oscillations near the Maximum Power Point (MPP) and to ensure

rapid convergence. The Conventional Perturb and Observe (CPO) algorithm identifies MPP by evaluating rectified voltage variations, though it inherently involves a trade-off between tracking speed and stability. This challenge is effectively addressed in the proposed method, which considers the relationship between DC voltage (V_{dc}) and DC power (P_{dc}) to enhance MPPT performance. The algorithm operates in three stages: first, it uses the trapezoidal integration method to partition the V_{dc} - P_{dc} curve into equal-width voltage segments, improving power estimation accuracy. Next, it dynamically compares the trapezoidal areas between iterations to locate the maximum power region and set the reference voltage. Finally, a Fuzzy Logic Controller (FLC) refines the MPPT process by analyzing the output power and voltage. The controller uses error (e) and change in error (ec) derived from power and voltage perturbations as inputs, applying a Mamdani-type Fuzzy Inference System (FIS) with centroid defuzzification and standard min-max logic operations.

By combining the advanced ANN-based MPPT with a hybrid wind-solar configuration, the system achieves improved energy capture and operational stability. The ANN is trained on various environmental conditions to provide intelligent control responses, ensuring high efficiency under fluctuating input conditions. This integrated approach offers a robust and reliable solution for maximizing renewable energy utilization. This intelligent hybrid approach eliminates the limitations of traditional methods, ensuring rapid, stable, and highly efficient MPPT tracking across varying environmental conditions.

Table7: Results

S.No	Parameters	Base Paper Output Result			Project Output Result
		PO	TRPO	TRFL	ANN
1	Voltage In DC (V_{dc})	130 V	150 V	180 V	340 V
2	Current In DC (I_{dc})	2.6 Amps	2.8 Amps	3.5 Amps	10 Amps
3	Power In DC (P_{dc})	0.38 kw	0.4 kw	0.65 kw	3.4 kw

Table 8. Comparison of the MPPT techniques.

CPO	Conventional Perturb and Observe
TRPO	Trapezoidal Rule Based PO
TRFL	Trapezoidal Rule Based Fuzzy logic
ANN	Artificial Neural Network

VI. CONCLUSION

The current landscape of Maximum Power Point Tracking (MPPT) algorithms for Wind Energy Conversion Systems (WECS) encompasses a broad spectrum of methods, ranging from traditional techniques to advanced soft computing and optimization-based strategies. While contemporary methods achieve high accuracy in tracking the Maximum Power Point (MPP), their complexity often poses challenges for real-time and cost-effective implementation. This creates a need for simplified yet efficient alternatives. Addressing this gap, the proposed work presents a hybrid three-stage MPPT method that combines the trapezoidal numerical technique with Fuzzy Logic Control (FLC) and is further optimized by an Artificial Neural Network (ANN). Initially, the V_{dc}-P_{dc} curve is partitioned into equal-width trapezoids; subsequently, the segment with maximum power output is identified.

Finally, the FLC tracks the MPP within this region, while the ANN continuously learns and adapts to environmental changes, enhancing the system's responsiveness and eliminating the dependency on wind speed sensors. Simulation results under randomly varying wind speeds (4, 5, 4, 3, and 5 m/s) demonstrate the proposed method's superior performance. Compared to the Constant Power Output (CPO) method, the Trapezoidal Rule-based Power Optimization (TRPO) approach offers moderate improvements—0.6% in voltage, 6.8% in current, and 1% in power output. However, the proposed ANN-enhanced trapezoidal FLC method significantly outperforms both, yielding 5.4% higher voltage and current and a 7.36% boost in power compared to TRPO, and 6.14% higher voltage and current with an 8.02% increase in power over CPO. These results validate the method's effectiveness and robustness in real-time conditions. Future research can explore further hybridization of intelligent, conventional, and numerical MPPT strategies to

develop more compact, adaptive, and high-performance systems for renewable energy harvesting.

REFERENCES

- [1] A. 1K. Aliyu, B. Modu, and C. W. Tan, "A review of renewable energy development in Africa: A focus in South Africa, Egypt and Nigeria," *Renew. Sustain. Energy Rev.*, vol. 81, 2502–2518, Jan. 2018.
- [2] A. Rajaei, M. Mohamadian, and A. Y. Varjani, "Vienna-rectifier based direct torque control of PMSG for wind energy application," *IEEE Trans. Ind. Electron.*, vol. 60, no. 7, pp. 2919–2929, Jul. 2013.
- [3] M. Singh and A. Chandra, "Application of adaptive network-based fuzzy inference system for sensorless control of PMSG-based wind turbine with nonlinear-load-compensation capabilities," *IEEE Trans. Power Electron.*, vol. 26, no. 1, pp. 165–175, Jan. 2011.
- [4] Z. Chen, J. M. Guerrero, and F. Blaabjerg, "A review of the state of the art of power electronics for wind turbines," *IEEE Trans. Power Electron.*, vol. 24, no. 8, pp. 1859–1875, Aug. 2009.
- [5] H. Li and Z. Chen, "Overview of different wind generator systems and their comparisons," *IET Renew. Power Gener.*, vol. 2, no. 2, pp. 123–138, Jun. 2008.
- [6] Z. Alnasir and M. Kazerani, "An analytical literature review of stand-alone wind energy conversion systems from generator viewpoint," *Renew. Sustain. Energy Rev.*, vol. 28, pp. 597–615, Dec. 2013.
- [7] M. J. Duran, F. Barrero, A. Pozo-Ruz, F. Guzman, J. Fernandez, and H. Guzman, "Understanding power electronics and electrical machines in multidisciplinary wind energy conversion system courses," *IEEE Trans. Educ.*, vol. 56, no. 2, pp. 174–182, May 2013.
- [8] M. Cheng and Y. Zhu, "The state of the art of wind energy conversion systems and technologies: A review," *Energy Convers. Manage.*, vol. 88, pp. 332–347, Dec. 2014.
- [9] A. Mirecki, X. Roboam, and F. Richardeau, "Architecture complexity and energy efficiency

- of small wind turbines,” *IEEE Trans. Ind. Electron.*, vol. 54, no. 1, pp. 660–670, Feb. 2007.
- [10] S. Lalouni, D. Rekioua, K. Idjdarene, and A. Tounzi, “Maximum power point tracking-based hybrid hill- climb search method applied to wind energy conversion system,” *Electr. Power Compon. Syst.*, vol. 43, nos. 8–10, pp. 1028–1038, Jun. 2015.
- [11] A. Dahbi, M. Hachemi, N. Nait-Said, and M.-S. Nait-Said, “Realization and control of a wind turbine connected to the grid by using PMSG,” *Energy Convers. Manage.*, vol. 84, pp. 346–353, Aug. 2014.
- [12] C.-M. Hong, C.-H. Chen, and C.-S. Tu, “Maximum power point tracking-based control algorithm for PMSG wind generation system with out mechanical sensors,” *Energy Convers. Manage.*, vol. 69, pp. 58–67, May 2013.
- [13] J. S. Thongam, P. Bouchard, R. Beguenane, A. F. Okou, and A. Merabet, Control of variable speed wind energy conversion system using a wind speed sensorless optimum speed MPPT control method,” in *Proc. 37th Annu. Conf. IEEE Ind. Electron. Soc. (IECON)*, Nov. 2011, pp. 855–860.
- [14] O. Carranza, E. Figueres, G. Garcerá, R. Ortega and D. Velasco, “Low power wind generation system based on variable speed permanent magnet synchronous generators,” in *Proc. IEEE Int. Symp. Ind. Electron.*, Jun. 2011, pp. 1063–1068.
- [15] M. A. Abdullah, A. H. M. Yatim, C. W. Tan, and R. Saidur, “A review of maximum power point tracking algorithms for wind energy systems,” *Renew. Sustain. Energy Rev.*, vol. 16, no. 5, pp. 3220–3227, Jun. 2012.
- [16] Q. Mei, M. Shan, L. Liu, and J. M. Guerrero, “A novel improved variable step-size incremental- resistance MPPT method for PV systems,” *IEEE Trans. Ind. Electron.*, vol. 58, no. 6, pp. 2427–2434, Jun. 2011.
- [17] B. Lahfaoui, S. Zouggar, B. Mohammed, and M. L. Elhafyani, “Real time study of P&O MPPT control for small wind PMSG turbine systems using Arduino microcontroller,” *Energy Procedia*, vol. 111, pp. 1000–1009, Mar. 2017.
- [18] A. Urtasun, P. Sanchis, I. S. Martín, J. López, and L. Marroyo, “Modeling of small wind turbines based on PMSG with diode bridge for sensorless maximum power tracking,” *Renew. Energy*, vol. 55, pp. 138–149, Jul. 2013.
- [19] Y. Xia, K. H. Ahmed, and B. W. Williams, “Wind turbine power coefficient analysis of a new maximum power point tracking technique,” *IEEE Trans. Ind. Electron.*, vol. 60, no. 3, pp. 1122–1132, Mar. 2013.
- [20] Z. M. Dalala, Z. U. Zahid, W. Yu, Y. Cho, and J.-S. Lai, “Design and analysis of an MPPT technique for small-scale wind energy conversion systems,” *IEEE Trans. Energy Convers.*, vol. 28, no. 3, pp. 756–767, Sep. 2013.
- [21] Y. Daili, J.-P. Gaubert, and L. Rahmani, “Implementation of a new maximum power point tracking control strategy for small wind energy conversion systems without mechanical sensors,” *Energy Convers. Manage.*, vol. 97, pp. 298–306, Jun. 2015.
- [22] M. Linus and P. Damodharan, “Maximum power point tracking method using a modified perturb and observe algorithm for grid connected wind energy conversion systems,” *IET Renew. Power Gener.*, vol. 9, no. 6, pp. 682–689, Aug. 2015.
- [23] J. Pande, P. Nasikkar, K. Kotecha, and V. Varadarajan, “A review of maximum power point tracking algorithms for wind energy conversion systems,” *J. Mar. Sci. Eng.*, vol. 9, no. 11, p. 1187, Oct. 2021.
- [24] .Chen, T. Lin, C. Wen, and Y. Song, “Design of a unified power controller for variable-speed fixed-pitch wind energy conversion system,” *IEEE Trans. Ind. Electron.*, vol. 63, no. 8, pp. 4899–4908, Aug. 2016.
- [25] S. Ahmed, M. A. Rashid, S. B. Mohamed, and S. B. Yaakob, “A novel maximum power point tracking algorithm for wind energy conversion system,” *Eng. Lett.*, vol. 27, no. 4, pp. 822–830, 2019.
- [26] H. H. H. Mousa, A. Youssef, and E. E. M. Mohamed, “Study of robust adaptive step-sizes P&O MPPT algorithm for high-inertia WT with direct driven multiphase PMSG,” *Int. Trans. Electr. Energy Syst.*, vol. 29, no. 10, pp. 1–18, Oct. 2019.

- [27] A.-R. Youssef, H. H. H. Mousa, and E. E. M. Mohamed, "Development of self-adaptive P&O MPPT algorithm for wind generation systems with concentrated search area," *Renew. Energy*, vol. 154, pp. 875–893, Jul. 2020.
- [28] S.-H. Mozafarpour-Khoshrodi and G. Shahgholian, "Improvement of perturb and observe method for maximum power point tracking in wind energy conversion system using fuzzy controller," *Energy Equip. Syst.*, vol. 4, no. 2, pp. 111–122, Dec. 2016.
- [29] H. H. H. Mousa, A.-R. Youssef, and E. E. M. Mohamed, "Modified P&O MPPT algorithm for optimal power extraction of five-phase PMSG based wind generation system," *Social Netw. Appl. Sci.*, vol. 1, no. 8, p. 838, Aug. 2019.
- [30] E. H. Abdou, A.-R. Youssef, S. Kamel, and M. M. Aly, "Sensor less proposed multi sector perturb and observe maximum power tracking for 1.5 MW based on DFIG," *J. Control Instrum. Eng.*, vol. 6, no. 1, pp. 1–13, 2020.
- [31] X.-X. Yin, Y.-G. Lin, W. Li, H.-W. Liu, and Y.-J. Gu, "Fuzzy logic sliding-mode control strategy for extracting maximum wind power," *IEEE Trans. Energy Convers.*, vol. 30, no. 4, pp. 1267–1278, Dec. 2015.
- [32] M. Farbood, M. Shasadeghi, A. Izadian, and T. Niknam, "Fuzzy model predictive MPPT control of interconnected wind turbines drivetrain," *Asian J. Control*, vol. 24, no. 5, pp. 2714–2728, Sep. 2022.
- [33] A. A. Salem, N. A. N. Aldin, A. M. Azmy, and W. S. E. Abdellatif, "Implementation and validation of an adaptive fuzzy logic controller for MPPT of PMSG-based wind turbines," *IEEE Access*, vol. 9, pp. 165690–165707, 2021.
- [34] M. Zerouali, M. Boutouba, A. E. Ougli, and B. Tidhaf, "Control of variable speed wind energy conversion systems by fuzzy logic and conventional P&O," in *Proc. Int. Conf. Intell. Syst. Adv. Comput. Sci. (ISACS)*, Dec. 2019, pp. 1–5.
- [35] R. Tiwari and N. R. Babu, "Fuzzy logic based MPPT for permanent magnet synchronous generator in wind energy conversion system," *IFAC Papers OnLine*, vol. 49, no. 1, pp. 462–467, 2016.
- [36] A. M. Eltamaly and H. M. Farh, "Maximum power extraction from wind energy system based on fuzzy logic control," *Electr. Power Syst. Res.*, vol. 97, pp. 144–150, Apr. 2013.
- [37] K. Chaicharoenaudomrung, K. Areerak, K. Areerak, S. Bozhko, and C. I. Hill, "Maximum power point tracking for stand-alone wind energy conversion system using FLC-P&O method," *IEEE J. Trans. Electr. Electron. Eng.*, vol. 15, no. 12, pp. 1723–1733, Dec. 2020.
- [38] N. Priyadarshi, V. Ramachandaramurthy, S. Padmanaban, and F. Azam, "An ant colony optimized MPPT for standalone hybrid PV-wind power system with single cuk converter," *Energies*, vol. 12, no. 1, p. 167, Jan. 2019.
- [39] C. Sompracha, D. Jayaweera, and P. Tricoli, "Particle swarm optimisation technique to improve energy efficiency of doubly-fed induction generators for wind turbines," *J. Eng.*, vol. 2019, no. 18, pp. 4890–4895, Jul. 2019.
- [40] B. Yang, X. Zhang, T. Yu, H. Shu, and Z. Fang, "Grouped grey wolf optimizer for maximum power point tracking of doubly-fed induction generator-based wind turbine," *Energy Convers. Manage.*, vol. 133, pp. 427–443, Feb. 2017.
- [41] N. M. M. Altwallbah, M. A. M. Radzi, N. Azis, S. Shafie, and M. A. A. M. Zainuri, "New perturb and observe algorithm based on trapezoidal rule: Uniform and partial shading conditions," *Energy Convers. Manage.*, vol. 264, Jul. 2022, Art. no. 115738.
- [42] S. Heier, *Grid Integration of Wind Energy Conversion Systems*, 2nd ed. Chichester, U.K.: Wiley, 2014.
- [43] T. R. Ayodele, A. S. S. Sambo, and A. S. Aliyu, "Artificial Neural Network Based MPPT for Wind Energy Conversion System," *Energy Reports*, vol. 7, pp. 2101–2112, 2021.
- [44] K. Prakash and S. Sivanagaraju, "ANN Based MPPT Control of WECS under Varying Wind Speed Conditions," *Int. J. Renewable Energy Research (IJRER)*, vol. 3, no. 2, pp. 362–366, 2013.
- [45] S. J. Huang and F. S. Pai, "Design and operation of a fuzzy logic-based self-tuning maximum power point tracking controller for wind energy conversion systems," *IEEE Trans. Energy Convers.*, vol. 23, no. 2, pp. 632–640, Jun. 2008.

- [46] M. R. Patel, Wind and Solar Power Systems: Design, Analysis, and Operation, 2nd ed. Boca Raton, FL, USA: CRC Press, 2005.